

## Low-energy electric and magnetic dipole excitations in $^{52}\text{Cr}$ \*

N. Tsoneva<sup>1,2</sup>, M. Bhike<sup>3</sup>, Krishichayan<sup>3</sup>, H. Lenske<sup>1,4</sup>, G. Rusev<sup>5</sup>, A.P. Tonchev<sup>6</sup>, and W. Tornow<sup>3</sup>

<sup>1</sup>Institut für Theoretische Physik, Universität Gießen; <sup>2</sup>INRNE, 1784 Sofia, Bulgaria; <sup>3</sup>Department of Physics, Duke University, Durham, NC 27708, and, Triangle Universities Nuclear Laboratory, Durham, NC 27708; <sup>4</sup>GSI Darmstadt;

<sup>5</sup>Chemistry Division, Los Alamos National Laboratory, Los Alamos, NM 87545; <sup>6</sup>Physics Division, Livermore Lawrence National Laboratory, Livermore, CA 94550

Electric and magnetic dipole strengths, below and around the neutron-emission threshold of  $^{52}\text{Cr}$  ( $S_n = 12.034$  MeV), are studied in the framework of the nuclear energy-density-functional (EDF) theory and an extended version of the Quasiparticle-Phonon Model (QPM) [1, 2]. The QPM results presented here are consistent with our previous analyses of  $E1$ ,  $E2$ , and  $M1$  excitations in various nuclei [1, 2, 3, 4, 5, 6, 7]. The theoretical results are compared with measurements from  $^{52}\text{Cr}(\gamma, \gamma')$  photon scattering experiments which have been performed using the nearly monoenergetic, 100% linear polarized photon beams produced at the HI $\gamma$ S facility of TUNL [8]. Twenty beam energies have been used to cover the energy range from 5.0 to 9.5 MeV and to uniquely identify and measure the dipole states in  $^{52}\text{Cr}$ . Twenty six dipole excitations were identified and their parity quantum values were unambiguously determined from the measured azimuthal intensity asymmetry of nuclear resonance fluorescence transitions. For the analysis of the experiment a sufficiently large QPM model basis, constructed of up to three-phonon (microscopically described) configurations with  $J^\pi$  from  $1^\pm$  to  $6^\pm$  and excitation energies  $E_x$  up to 9.8 MeV is implemented [8]. From EDF mean-field calculations we derive that the  $^{52}\text{Cr}$  nucleus exhibits a neutron skin with a thickness of  $\delta r = 0.056$  fm. As a result, the first QRPA  $1^-$  state with excitation energy  $E_x = 8.366$  MeV, and the second QRPA  $1^-$  state with excitation energy  $E_x = 9.473$  MeV are almost pure neutron two-quasiparticle states, where the major contribution is due to transitions from weakly bound neutron orbitals. Further analysis of transition densities of these states shows features typical for skin nuclei [2, 6]. Thus, the QRPA  $1^-$  excitations below  $\sim 9.5$  MeV in  $^{52}\text{Cr}$  could be associated with a genuine Pygmy Dipole Resonance (PDR) mode [1, 2, 9]. The total PDR strength obtained from the QRPA calculations is  $\Sigma_{0\text{MeV}}^{9.5\text{MeV}} B(E1; g.s. \rightarrow 1^-_{\text{PDR}})_{\text{QRPA}} \uparrow = 13 \times 10^{-3} \text{ e}^2\text{fm}^2$  which exhausts about 0.1% of the Energy-Weighted Sum Rule (EWSR)[10]. As the excitation energy is increased, the isovector contribution to the dipole strength increases, and the state vectors show an increase of the out-of-phase neutron to proton contribution which is generally associated with the Giant Dipole Resonance (GDR) [2, 6].

Theoretically, it is clear that the QRPA is unable to account for higher multi-particle-multi-hole correlations and interactions resulting from core polarization effects [11]. The later could induce dynamical effects related to re-

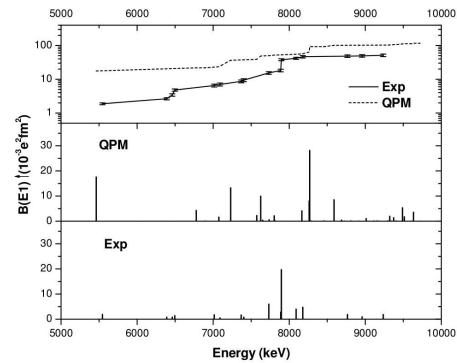


Figure 1: (color online) Distribution of observed  $B(E1) \uparrow$  strength for resonantly excited states between 5.1 and 9.5 MeV in  $^{52}\text{Cr}$  is compared with values obtained from three-phonon QPM calculations. A comparison of the measured and calculated QPM cumulative  $E1$  strength is shown in the upper panel.

distribution of strength, and strongly affect the gross and fine structure of dipole strength functions. By comparing the QRPA with the multi-phonon QPM calculations, it is seen that the pure two-quasiparticle QRPA strengths in the PDR region is strongly fragmented over many  $1^-$  excited states, once the coupling to multiphonon configurations takes place. Thus, the lowest-lying  $1^-$  state, which is without a QRPA counterpart, is predominantly given by a two-phonon quadrupole-octupole excitation of the  $[2_1^+ \otimes 3_1^-]_{1^-}$  configuration, which accounts for  $\approx 75\%$  of the QPM wave function [8]. The strongest QPM  $1^-_{\text{max}}$  state in the energy range below 9.8 MeV is located at  $E_{\text{QPM}} = 8.270$  MeV and the corresponding transition probability is  $B(E1; g.s. \rightarrow 1^-_{\text{max}})_{\text{QPM}} \uparrow = 28.14 \times 10^{-3} \text{ e}^2\text{fm}^2$ . The theoretical results compare well with the experimental findings, which give for this state  $E_{\text{exp}} = 7.897$  MeV and  $B(E1; g.s. \rightarrow 1^-_{\text{max}})_{\text{QPM}} \uparrow = 19.7(10) \times 10^{-3} \text{ e}^2\text{fm}^2$ , and also with the results of Pai *et al.* [12]. The QPM calculations indicate that the  $1^-_{\text{max}}$  state contains contributions of the low-energy tail of the GDR, which is the reason for the strong  $B(E1)$  transition rate.

The comparison between the measurements and the QPM  $E1$  spectral distribution and the cumulative  $B(E1)$  strength in  $^{52}\text{Cr}$  is presented in Fig. 1. In general, the shape of the QPM cumulative  $B(E1)$  strength as well as the  $1^-$  level distribution are found to be in a good agreement with the experimental data. In particular, for the whole measured energy range  $E_x = 5.1 - 9.5$  MeV the

\* Work supported by the HIC for FAIR, GSI-JLU Giessen collaboration agreement, the U.S. Department of Energy Grant No DE-FG02-97ER41033 and BMBF grant 05P12RGFTE.

QPM calculations predict a summed  $B(E1)$  strength of  $\sum B(E1)_{QPM} \uparrow = 111.4 \times 10^{-3} e^2 fm^2$ . In comparison, the experiment finds  $\sum B(E1)_{exp} \uparrow = 51.2(16) \times 10^{-3} e^2 fm^2$ , approximately a factor of two less strength.. The observed difference between the measured and calculated total  $B(E1)$  values could be related to experimental sensitivity limits and branchings to excited states, which are unaccounted for by the existing dipole data in  $^{52}Cr$ .

The main aim of this work is to perform unambiguous parity assignments of the low-energy dipole states in  $^{52}Cr$  and a precise separation between electric  $E1$  and magnetic  $M1$  excitations. Experimentally it is achieved in measurements of azimuthal asymmetries of NRF  $\gamma$ -rays using a 100% linearly polarized and quasi-monochromatic photon beam [3, 4, 8]. The  $M1$  data are analysed theoretically by three phonon QPM calculations. In the determination of the nuclear magnetic transition moments a quenched effective spin-magnetic factor  $g_{eff}^s = 0.8g_{bare}^s$  is used, where  $g_{bare}^s$  denotes the bare spin-magnetic moment. The quenching factor agrees very well with accepted QPM values [11], shell-model calculations and experimental data [13, 14, 15]. A reliable description of the fragmentation pattern of the magnetic dipole response function is important for understanding the spin dynamics of the nucleus. The analysis of the QRPA  $M1$  strength of  $1^+$  excitations with energies up to  $E_x = 20$  MeV indicates that this part of the spectrum is mostly due to transitions of spin-flip type related to the neutron and proton  $1f_{7/2} \rightarrow 1f_{5/2}$  two-quasiparticle components, respectively [8]. The detailed studies of the  $M1$  response function, performed by three-phonon QPM calculations, show that the coupling of natural parity phonons to multi-phonon  $1^+$  states induces additional orbital contribution to the  $M1$  transitions. Consequently, the observed  $M1$  strength at excitation energies between 5 and 10 MeV contains an orbital part of about 11%. In comparison the QRPA calculations provide us a very small amount of orbital  $M1$  strength of about 3.3 % of the total QRPA  $B(M1)$  transition probability, up to  $E_x = 20$  MeV [8]. The total QPM  $M1$  strength summed over  $1^+$  states from  $E_x = 5$  to 9.5 MeV can be compared directly with the present data. The results are presented in Fig. 2. The theoretical findings give  $\sum_{5MeV}^{9.5MeV} B(M1)_{QPM} \uparrow = 3.1 \mu_N^2$ , which is in good agreement with the experimental value of  $\sum_{5MeV}^{9.5MeV} B(M1)_{exp} \uparrow = 2.94(9) \mu_N^2$  [8].

The observation of the spin-flip  $M1$  resonance structure around 9.1 MeV in  $^{52}Cr$  has been discussed along with the systematics of dipole excitation transition strength distributions in  $fp$ -shell nuclei [8]. Such concentration of  $M1$  strength around 9.2 MeV is confirmed in the three-phonon QPM calculations and explained as fragmented spin-flip  $1^+$  excitations [8].

In conclusion, a common observation is that the QRPA is unable to describe the low-energy  $E1$  and  $M1$  spectral distributions. However, a detailed explanation could be obtained in multi-phonon model like the three-phonon QPM, which can describe well the observed experimentally fragmentation pattern of the low-energy dipole strength. The

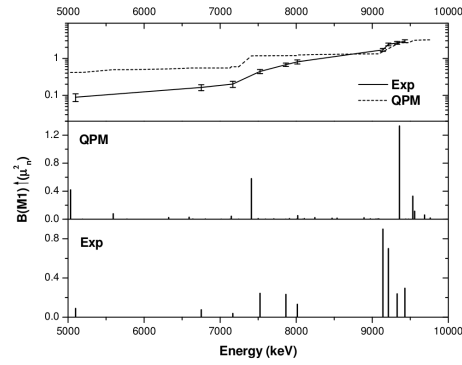


Figure 2: (color online) Distribution of observed  $B(M1) \uparrow$  strength in  $^{52}Cr$  in the energy range between 5.1 and 9.5 MeV is compared with the values obtained from three-phonon QPM calculations. A comparison of the measured and calculated QPM cumulative  $M1$  strength is shown in the upper panel.

good agreement between the calculated and measured total  $M1$  strength is a signature that the quenching is handled reliably well in the chosen approximation. A better understanding could be achieved with more comprehensive knowledge of the nature of the intrinsic nuclear moments, meson-exchange currents and branching ratios from excited states, which might be of importance for further improvements. Supported by the U.S. Department of Energy Grant No DE-FG02-97ER41033 and BMBF grant 05P12RGFTE.

## References

- [1] N. Tsoneva, H. Lenske, Ch. Stoyanov, Phys. Lett. **B586**, 213 (2004) and refs. therein.
- [2] N. Tsoneva, H. Lenske, Phys. Rev. C **77**, 024321 (2008) and refs. therein.
- [3] A. Tonchev *et al.*, Phys. Rev. Lett. **104** 072501 (2010).
- [4] G. Rusev *et al.*, Phys. Rev. Lett. **110**, 022503 (2013).
- [5] N. Tsoneva, H. Lenske, Phys. Lett. **B695** 174 (2011).
- [6] R. Schwengner *et al.*, Phys. Rev. C **87**, 024306 (2013).
- [7] B. Özel-Tashenov *et al.*, Phys. Rev. C **90**, 024304 (2014).
- [8] Krishichayan, M. Bhike, W. Tornow, G. Rusev, A.P. Tonchev, N. Tsoneva, and H. Lenske, Phys. Rev. C submitted.
- [9] D. Savran, T. Aumann, and A. Zilges, Prog. Part. Nucl. Phys. **70**, 210 (2013).
- [10] B. L. Berman, At. Data Nucl. Data Tables **15**, 319 (1975).
- [11] V.G. Soloviev, *Theory of complex nuclei* (Oxford: Pergamon Press, 1976).
- [12] H. Pai *et al.*, Phys. Rev. C **88**, 054316 (2013).
- [13] P. von Neumann-Cosel *et al.*, Phys. Lett. **B443**, 1 (1998).
- [14] K. Langanke, G. Martinez-Pinedo, P. von Neumann-Cosel, A. Richter, Phys. Rev. Lett. **93**, 202501 (2004).
- [15] S.E. Koonin, D.J. Dean, K. Langanke, Annu. Rev. Nucl. Part. Sci. **47**, 403 (1997).